On Molecular Topological Characterization of Triangular and Rhombus Shaped Kekulene Tessellations

Arulperumjothi M[1], Savari Prabhu[2], Jia-bao Liu[3], Lakshmi V[2], and Manimozhi V[4]

[1]Saveetha Engineering College (Autonomous)
[2]Rajalakshmi Engineering College
[3]Anhui Xinhua University
[4]Panimalar Engineering College

July 20, 2022

Abstract

Cycloarenes are a particular category of polycyclic aromatic hydrocarbons that have intrigued the experimental world for decades owing to the distinctiveness of their atomic and electrical configurations. They are suitable venues for investigating fundamental problems of aromaticity, particularly those involving the π-electron distribution in complex aromatic structures. Cycloarenes have recently attracted much attention due to their distribution as analogs for graphene pores. Kekulene is the member of this family that has been studied the most. For decades, its electrical structure has been a source of contention. It's a doughnut-shaped chemical structure of circularly stacked benzene rings with interesting structural characteristics that lend themselves to experimental investigations like π-electron conjugation circuits. To predict their properties, topological characterization of such structures is required. This paper discusses two new series of big polycyclic compounds made by tessellating many kekulene doughnuts to make a hypothetical molecular belt with multiple cavities

On Molecular Topological Characterization of Triangular and Rhombus Shaped Kekulene Tessellations

M. Arulperumjothi[a,*], S. Prabhu[b], Jia-Bao Liu[c], V. Lakshmi[b], V. Manimozhi[d]

[a]Department of Mathematics, Saveetha Engineering College, Thandalam, Chennai 602105, India

[b]Department of Mathematics, Rajalakshmi Engineering College, Thandalam, Chennai 602105, India

[c]School of Mathematics and Physics, Anhui Jianzhu University, Hefei 230601, P.R. China

[d]Department of Mathematics, Panimalar Engineering College, Chennai 600123, India

July 19, 2022

Abstract

Cycloarenes are a particular category of polycyclic aromatic hydrocarbons that have intrigued the experimental world for decades owing to the distinctiveness of their atomic and electrical configurations. They are suitable venues for investigating fundamental problems of aromaticity, particularly those involving the π-electron distribution in complex aromatic structures. Cycloarenes have recently attracted much attention due to their distribution as analogues for graphene pores. Kekulene is the member of this family that has been studied the most. For decades, its electrical structure has been a source of contention. It's a doughnut-shaped chemical structure of circularly stacked benzene rings with interesting structural characteristics that lend themselves to experimental investigations like π-electron conjugation circuits. To predict their properties, topological characterization of such structures is required. This paper discusses two new series of big polycyclic compounds made by tessellating many kekulene doughnuts to make a hypothetical molecular belt with multiple cavities.

Keywords: Topological indices; molecular graph; convex cuts; kekulene.

1 Introduction

Polycyclic aromatic compounds have captivated researchers' attention in recent years since they are found in a variety of manufacturing chemicals and hence pose a threat to the environment as pollutants [42, 43]. These substances are long-lasting materials with a wide range of structures and toxicity, as well

---

*Corresponding author : marulperumjothi@gmail.com

as high melting and boiling temperatures and low water solubility and vapour pressure [42]. Electronics, pharmaceuticals, agricultural and photographic products, functional polymers, and liquid crystals have really shown attention in the chemical and bioactivities among those polycyclic aromatics [1]. Because several polycyclic aromatic compounds' derivatives are toxic as well as carcinogenic, various research has been conducted to analyse their influence on that ecosystem and create a remediation approach [1, 57]. Furthermore, due to the phenomena of superaromaticity attributed to macrocyclic extended conjugations, cycloarenes have garnered a strong interest. To comprehend superaromaticity, numerous theoretical techniques [11, 13, 25–27, 37, 38, 54, 58] including graph-relevant theoretical conjugated circuit methods were used to widen and extensively study the idea of aromaticity. Cycloarenes establish an intriguing class of polycyclic aromatic hydrocarbons that have been fascinated in the academic network for decades because of the singularity of their atomic and electronic structures [11, 26, 37, 54, 58]. They fill in as ideal stages to examine principal inquiries around the idea of aromaticity and, specifically, those related to the π-electron distribution in complex aromatic systems [26]. Recently, improved attention regarding cycloarenes has emerged since serving as models for graphene pores [9, 24, 55, 63].

The structure of the kekulene molecule, which comprises twelve annulated benzene rings and a central cavity, offers the tantalizing promise of enhanced stability with remarkable magnetic and magnetocaloric effects. Kekulene has revealed remarkable counter ring currents and magnetic characteristics using *ab initio* quantum chemical methodology [59]. Despite its exceptional physicochemical properties, this compound's utilization has been constrained for a decade owing to its complicated synthesis techniques [11]. This molecule is regularly called superbenzene because of its planar cyclic formation and D_{6h} symmetry [29]. It has inspired a wave of conceptual attention since it is seen as an appropriate model for considering conjugation circuits of π electrons, whether they delocalize locally in benzene rings or globally across the molecule [44]. Pozo et al. [46] demonstrated an appropriate direction for the kekulene synthesis using aryne chemistry, paving the way for large-scale manufacturing, which has prompted a huge interest. It has since been suggested as a contender for magnetic refrigeration [3]. It has also been presented as a suitable anode material for lithium-ion batteries due to its peculiar characteristics [28]. Consequently, a theoretical analysis of its new structure can reveal more information about its characteristics.

Breakthroughs in cycloarenes theory and experiment have necessitated the enumeration and characterization of these possible new compounds. Mathematical methods from group theory, combinatorial mathematics, and graph theory, as proven in a recent paper by Balasubramanian [7], can give powerful techniques for enumerating isomers and NMR signals of these compounds. Furthermore, quantitative molecular similarity and related principles play a significant role in supporting computer-aided drug discovery (CADD) methodologies, as do forecasts of toxicity potentials and potential findings of related

molecules [7]. Topological indices are a category of molecular parameters that provide quantitative measurements based on the underlying connectivity of the structure. However, their applications are still being studied and are not yet demonstrated [8, 33].
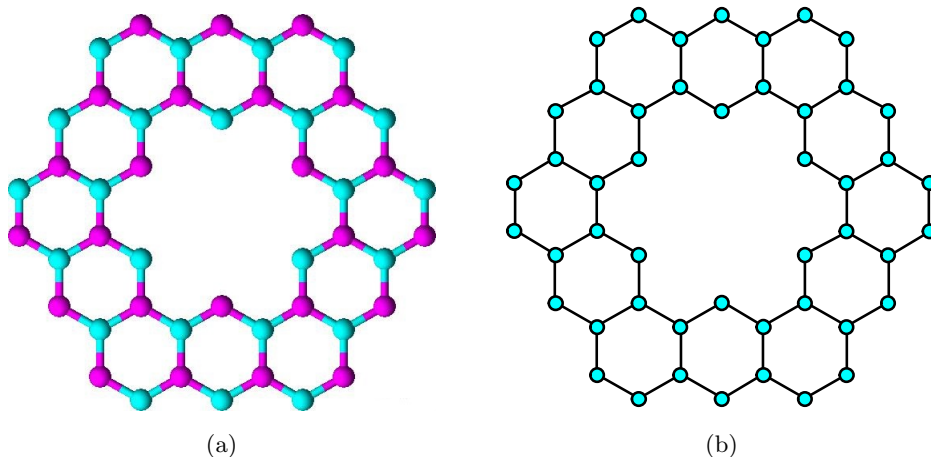

Figure 1: (a) Kekulene molecular structure (b) Molecular graph corresponding to kekulene molecular structure

Topological descriptors are numerical values derived from a molecular network in which each vertex indicates an atom, and each edge signifies a chemical link between them. Topological indices are molecular descriptors used to find a correlation model between chemical structure and the relevant physicochemical and biological activity [8,33]. These topological descriptors are part of a set of theoretical tools for describing the structural characteristics of these molecules. As a result, topological indices and their evolution have gotten much attention over the years. In the present study, we use theoretical and experimental studies to propose unique cut methods for obtaining exact expressions for the topological indices of triangle and rhombus tessellations of kekulenes, resulting in novel 2D molecular sheets with many cavities. We exploited strength-weighted graphs to derive the formula for various distance-based, degree-based, distance and degree-based, and bond additive-related topological indices.

2 Graph-Theoretical Concepts

A graph is an arranged pair (V, E), where V is known as the vertex set and E is known as the edge set. A non-negative number which shows the number of edges that enter the vertex v is known as the degree of a vertex $d_G(v)$, and the distance between two vertices u and v in a graph is the number of edges in a shortest or minimal path and $N_G(u)$ to be the set of vertices that adjacent to u. If $d_G(u, v) = d_H(u, v)$ then the subgraph H of G is supposed to be isometric, and if all the shortest path between any two vertices in G lies totally in H, at that point the subgraph H of G is said to be convex.

The cut method ended up being amazingly helpful when managing distance-based topological indices, which are thus among the focal ideas of chemical graph theory [34, 35]. It was frequently applied to benzenoid frameworks to compute distance-based topological indices effectively [4, 48].

Two edges $e = uv$ and $f = cd$ of a connected graph G are in Θ relation, $e\ \Theta\ f$, if

$$d_G(u, c) + d_G(v, d) \neq d_G(u, d) + d_G(v, c)$$

then it is known as Djoković-Winkler relation. The relation Θ is reflexive and symmetric, however not really transitive. Its transitive closure denoted by Θ^*. A significant group of graphs, which is firmly identified with connection Θ and incorporate numerous chemical graphs, are so-called partial cubes. Note that an associated graph is a incomplete partial cubes if and only if it is bipartite and $\Theta = \Theta^*$.

However, its transitive closure Θ^* forms an equivalence relation and partitions the edge set into many convex components. For any edge-cut F_i the quotient graph G/F_i is formed from the disconnected graph $G - F_i$, where the connected components (C_j^i, C_k^i) acts as the vertices in G/F_i and the edge set $E(G/F_i)$ is the set of edges where a vertex $x \in C_j^i$ is adjacent to a vertex $y \in C_k^i$ with $xy \in F_i$. A partition $\mathscr{E} = \{E_1, E_2, \ldots E_k\}$ of $E(G)$ is said to be coarser than $\mathscr{F}$ if each set E_i is the union of one or more Θ^*-classes of G.

The strength-weighted graph was at first presented in [4] and widely discussed in [5, 5, 6, 12, 30–32, 39, 47–51] as $G_{sw} = (G, (w_v, s_v), s_e)$, where the vertex-weight and vertex-strength are $w_v : V(G_{sw}) \to \mathbb{R}_0^+$, $s_v : V(G_{sw}) \to \mathbb{R}_0^+$ and the edge-strength capacity are $s_e : E(G_{sw}) \to \mathbb{R}_0^+$. For any edge $uv \in E(G)$, then the following sets:

$$N_u(e|G) = \{x \in V(G)|d_G(u, x) < d_G(v, x)\}, \ N_v(e|G) = \{x \in V(G)|d_G(v, x) < d_G(u, x)\}$$

In strength-weighted graph, $d_{G_{sw}}(u, v) = d_G(u, v)$, $d_{G_{sw}}(u, f) = d_G(u, f)$, $D_{G_{sw}}(e, f) = D_G(e, f)$, $N_u(e|G_{sw}) = N_u(e|G)$ and $M_u(e|G_{sw}) = M_u(e|G)$. for any edge $uv \in E(G_{sw})$, then the following sets:

$$n_u(e|G_{sw}) = \sum_{x \in N_u(e|G_{sw})} w_v(x),$$

$$m_u(e|G_{sw}) = \sum_{x \in N_u(e|G_{sw})} s_v(x) + \sum_{f \in M_u(e|G_{sw})} s_e(f)$$

$$t_u(e|G_{sw}) = n_u(e|G_{sw}) + m_u(e|G_{sw})$$

The computations of $n_v(e|G_{sw})$, $m_v(e|G_{sw})$ and $t_v(e|G_{sw})$ are analogous. The degree of a vertex u in G_{sw} is characterized as

$$d_{G_{sw}}(u) = 2s_v(u) + \sum_{x \in N_{G_{sw}}(u)} s_e(ux).$$

Theorem 1. *[4, 36] For a strength-weighted graph $G_{sw} = (G, (w_v, s_v), s_e)$, let $\mathscr{E} = \{E_1, E_2, \ldots E_k\}$ be a partition of $E(G)$ coarser than $\mathscr{F}$. Let TI represent various topological indices such as W, W_e, W_{ve}, Sz_v, Sz_e, Sz_{ev}, Sz_t, PI, S, and Gut. Then*

$$TI(G_{sw}) = \sum_{i=1}^{k} TI(G/E_i, (w_v^i, s_v^i), s_e^i)$$

where

- $w_v^i : V(G/E_i) \to \mathbb{R}^+$ *is defined by* $w_v^i(C) = \sum_{x \in C} w_v(x)$, *for all connected components* $C \in G/E_i$,

- $s_v^i : E(G/E_i) \to \mathbb{R}^+$ *is defined by* $s_v^i(C) = \sum_{xy \in C} s_e(xy) + \sum_{x \in C} s_v(x)$, *for all connected components* $C \in G/E_i$,

- $s_e^i : E(G/E_i) \to \mathbb{R}^+$ *is defined as the number of edges in* E_i *such that one end in* C *and the other end in* D, *for any two connected components* C *and* D *of* G/E_i.

The principal topological index was presented by Wiener and in these days realized as Wiener index. With time it became one of the most altogether considered topological index, both from the part of chemical applications and mathematical properties. Numerous varieties and types of Wiener index were presented and concentrated in literature. Many distinct variations of these topological indices have recently appeared in the literature, and in some cases they are collectively referred to as Szeged-like topological indices. Now, we properly characterize the above depicted topological indices for strength-weighted graph is shown in Table 1 with a connection that $TI(G_{sw}) = TI(G)$ when $w_v = 1$, $s_v = 0$ and $s_e = 1$.

Table 1: Topological indices for strength-weighted graph G_{sw}

Topological Indices	Mathematical Expressions
Wiener	$W(G_{sw}) = \displaystyle\sum_{\{u,v\} \subseteq V(G_{sw})} w_v(u)w_v(v)d_{G_{sw}}(u,v)$
Edge-Wiener	$W_e(G_{sw}) = \displaystyle\sum_{\{u,v\} \subseteq V(G_{sw})} s_v(u)\ s_v(v)\ d_{G_{sw}}(u,v)$ $+ \displaystyle\sum_{\{e,f\} \subseteq E(G_{sw})} s_e(e)\ s_e(f)\ D_{G_{sw}}(e,f)$ $+ \displaystyle\sum_{u \in V(G_{sw})}\sum_{f \in E(G_{sw})} s_v(u)\ s_e(f)\ d_{G_{sw}}(u,f)$
Vertex-edge-Wiener	$W_{ve}(G_{sw}) = \frac{1}{2}\left[\displaystyle\sum_{\{u,v\} \subseteq V(G_{sw})} \left\{w_v(u)\ s_v(v)\ +\ w_v(v)\ s_v(u)\right\} d_{G_{sw}}(u,v) \right.$ $\left. + \displaystyle\sum_{u \in V(G_{sw})}\sum_{f \in E(G_{sw})} w_v(u)\ s_e(f)\ d_{G_{sw}}(u,f) \right]$
Vertex-Szeged	$Sz_v(G_{sw}) = \displaystyle\sum_{e=uv \in E(G_{sw})} s_e(e)n_u(e|G_{sw})n_v(e|G_{sw})$
Edge-Szeged	$Sz_e(G_{sw}) = \displaystyle\sum_{e=uv \in E(G_{sw})} s_e(e)m_u(e|G_{sw})m_v(e|G_{sw})$
Edge-vertex-Szeged	$Sz_{ev}(G_{sw}) = \frac{1}{2} \displaystyle\sum_{e=uv \in E(G_{sw})} s_e(e)\left[n_u(e|G_{sw})m_v(e|G_{sw})+\right.$ $\left. n_v(e|G_{sw})m_u(e|G_{sw})\right]$
Total-Szeged	$Sz_t(G_{sw}) = Sz_v(G_{sw}) + Sz_e(G_{sw}) + 2Sz_{ev}(G_{sw})$
Padmakar-Ivan	$PI(G_{sw}) = \displaystyle\sum_{e=uv \in E(G_{sw})} s_e(e)\left[m_u(e|G_{sw}) + m_v(e|G_{sw})\right]$
Schultz	$S(G_{sw}) = \displaystyle\sum_{\{u,v\} \subseteq V(G_{sw})} \left[w_v(v)d_{G_{sw}}(u) + w_v(u)d_{G_{sw}}(v)\right]d_{G_{sw}}(u,v)$
Gutman	$Gut(G_{sw}) = \displaystyle\sum_{\{u,v\} \subseteq V(G_{sw})} d_{G_{sw}}(u)d_{G_{sw}}(v)d_{G_{sw}}(u,v)$

Degree-based indices are a class of molecular descriptors that are predicated on the graph's degree parameter and have interesting chemical applications. The Randić index [53] has to be the most important degree-based index for correlating alkane chemical characteristics such as boiling temperatures, chromatographic retention periods, and formation enthalpies. Other indices, such as Zagreb variations, forgotten, and geometric arithmetic indices [14, 15, 45], have a high degree of predictability and hence aid in the development of multi-linear regression models for future investigation of the compound. Variants of irregularity measures provide a numerical measure of molecular graph irregularity [2]. In [19, 22, 33, 64], the significance of such indices and potential utilization in the chemical industry were discussed. Some of the degree-based topological indices are listed in Table 2.

Table 2: Degree based topological indices

Topological Indices	Mathematical Expressions
Randić [10, 52]	$R(G) = \sum\limits_{uv \in E(G)} \frac{1}{\sqrt{d(u)d(v)}}$
Reciprocal Randić [17]	$RR(G) = \sum\limits_{uv \in E(G)} \sqrt{d(u)d(v)}$
Reduced reciprocal Randić [41]	$RRR(G) = \sum\limits_{uv \in E(G)} \sqrt{(d(u)-1)(d(v)-1)}$
First Zagreb [21]	$M_1(G) = \sum\limits_{u \in V(G)} d(u)^2$
Second Zagreb [21]	$M_2(G) = \sum\limits_{uv \in E(G)} d(u)d(v)$
Reduced second Zagreb [20]	$RM_2(G) = \sum\limits_{uv \in E(G)} (d(u)-1)(d(v)-1)$
Hyper Zagerb [56]	$HM(G) = \sum\limits_{uv \in E(G)} [d(u)+d(v)]^2$
Augmented Zagerb [18]	$AZ(G) = \sum\limits_{uv \in E(G)} \left(\frac{d(u)d(v)}{d(u)+d(v)-2}\right)^3$
Atom bond connectivity [15]	$ABC(G) = \sum\limits_{uv \in E(G)} \sqrt{\frac{d(u)+d(v)-2}{d(u)d(v)}}$
Harmonic [16]	$H(G) = \sum\limits_{uv \in E(G)} \frac{2}{d(u)+d(v)}$
Sum-connectivity [67]	$SC(G) = \sum\limits_{uv \in E(G)} \frac{1}{\sqrt{d(u)+d(v)}}$
Geometric arithmetic [61]	$GA(G) = \sum\limits_{uv \in E(G)} 2\left(\frac{\sqrt{d(u)d(v)}}{d(u)+d(v)}\right)$
Inverse sum indeg [60]	$ISI(G) = \sum\limits_{uv \in E(G)} \left(\frac{d(u)d(v)}{d(u)+d(v)}\right)$
First multiple Zagreb [66]	$PM_1(G) = \prod\limits_{uv \in E(G)} [d(u)+d(v)]$
Second multiple Zagreb [66]	$PM_2(G) = \prod\limits_{uv \in E(G)} [d(u) \times d(v)]$

3   Results

Polycyclics have been the topic of extensive theoretical and empirical investigation considering to their importance in numerous disciplines of science, such as organic photovoltaics [40], electronics [62], and optoelectronic devices [65]. These are made exclusively of concised hexagonal rings, either by circumscribing the benzene rings to increase the size of the base molecule or by confining the base molecule into dimers, trimers, and oligomers [23]. In this section, we concentrate on two PAHs with hollow spaces that are made using kekulene structures in a methodical way. Figure 1 depicts the fundamental chemical structure

of the kekulene molecule, which may be rearranged in a collection of ways to produce new sequence of massive PAHs. In this section, we discuss the triangular and rhombus shaped kekulene tessellation.

Theorem 2. *Let G be a triangular tessellation of kekulene system $TK(n)$. Then,*

(i) $W(G) = 3(162n^5 + 1485n^4 + 3916n^3 + 2925n^2 + 700n + 36)/4.$

(ii) $W_e(G) = 216n^5 + 1818n^4 + 4186n^3 + 2181n^2 + 455n + 12.$

(iii) $W_{ve}(G) = (648n^5 + 5697n^4 + 14074n^3 + 8967n^2 + 1934n + 72)/4.$

(iv) $Sz_v(G) = 3(540n^6 + 6051n^5 + 23520n^4 + 37055n^3 + 20120n^2 + 4534n + 180)/10.$

(v) $Sz_e(G) = 6(240n^6 + 2514n^5 + 9000n^4 + 12300n^3 + 4425n^2 + 1001n + 20)/5.$

(vi) $Sz_{ev}(G) = (432n^6 + 4683n^5 + 17484n^4 + 25745n^3 + 11724n^2 + 2500n + 72)/2.$

(vii) $Sz_t(G) = (8820n^6 + 95151n^5 + 353400n^4 + 516215n^3 + 230700n^2 + 50614n + 1500)/10.$

(viii) $PI(G) = 8(18n^4 + 124n^3 + 228n^2 + 47n + 3).$

(ix) $S(G) = 648n^5 + 5805n^4 + 14848n^3 + 10479n^2 + 2384n + 108.$

(x) $Gut(G) = 12(72n^5 + 630n^4 + 1562n^3 + 1038n^2 + 225n + 9).$

Proof. The number of vertices and edges of $TK(n)$ are respectively given by $9n^2+33n+6$ and $12n^2+42n+6$. Let $\{HZ_i : 1 \leq i \leq 4\}$ be the horizontal zigzag cuts which are Θ^*-classes, and $\{AZ_i : 1 \leq i \leq 4\}$, $\{OZ_i : 1 \leq i \leq 4\}$ be the acute zigzag and obtuse zigzag cuts produced by spinning the horizontal zigzag cuts by $60°$ and $120°$ in the anticlockwise direction and the same is depicted in Figure 2. Let $\{VC_i : 1 \leq i \leq 4\}, VM, \{VC'_i : 1 \leq i \leq 4\}, \{AC_i : 1 \leq i \leq 4\}, AM, \{AC'_i : 1 \leq i \leq 4\}, \{OC_i : 1 \leq i \leq 4\}$, OM and $\{OC'_i : 1 \leq i \leq 4\}$ be the various Θ-classes as depicted in Figure 3.

We only address all the above said cuts for $TK(n)$ once and account it 3 times in the computation procedure because of symmetry. We should also remark that the strength weighted quotient graphs for $\{HZ_i : 1 \leq i \leq n\}$, $\{AZ_i : 1 \leq i \leq n\}$, and $\{OZ_i : 1 \leq i \leq n\}$ are all isomorphic to Figure 2(d). Similarly, the quotient graphs for the Θ-classes VZ_{1i}, VZ'_{1i}, AC_{1i}, AC'_{1i}, OC_{1i}, and OC'_{1i}, where $1 \leq i \leq n$ along with their edge strengths are given in Figure 3(d) and corresponding strength-weigthted values are given in the Table 3. Also, the quotient graphs along with their edge strengths for middle Θ-classes VM, AM, and OM are given in Figure 3(e).

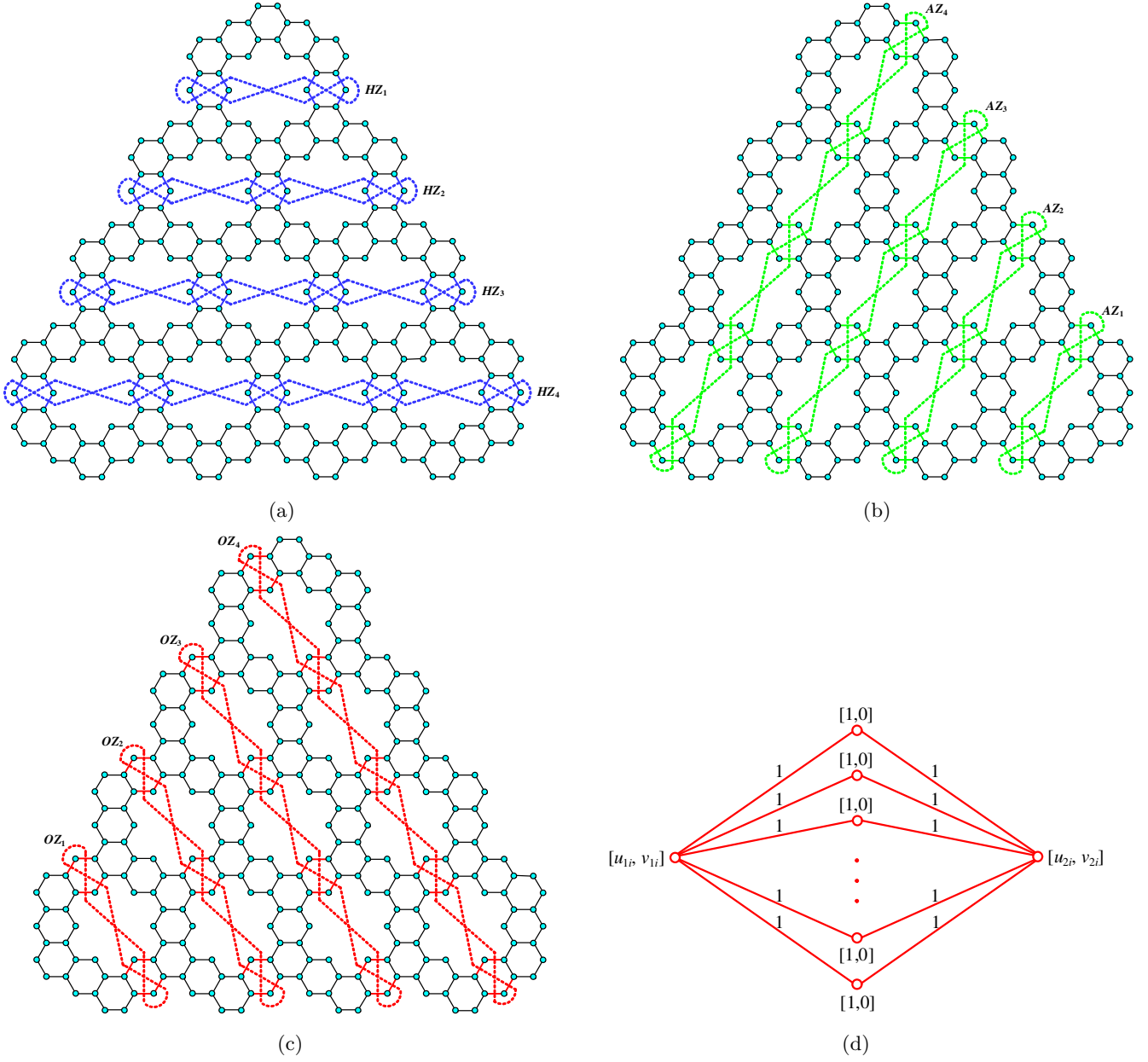Figure 2: Θ^*-classes of kekulene structure (a) Horizontal zigzag; (b) Acute zigzag; (c) Obtuse zigzag; (d) Quotient graph of zigzag cuts for the range $1 \le i \le n$
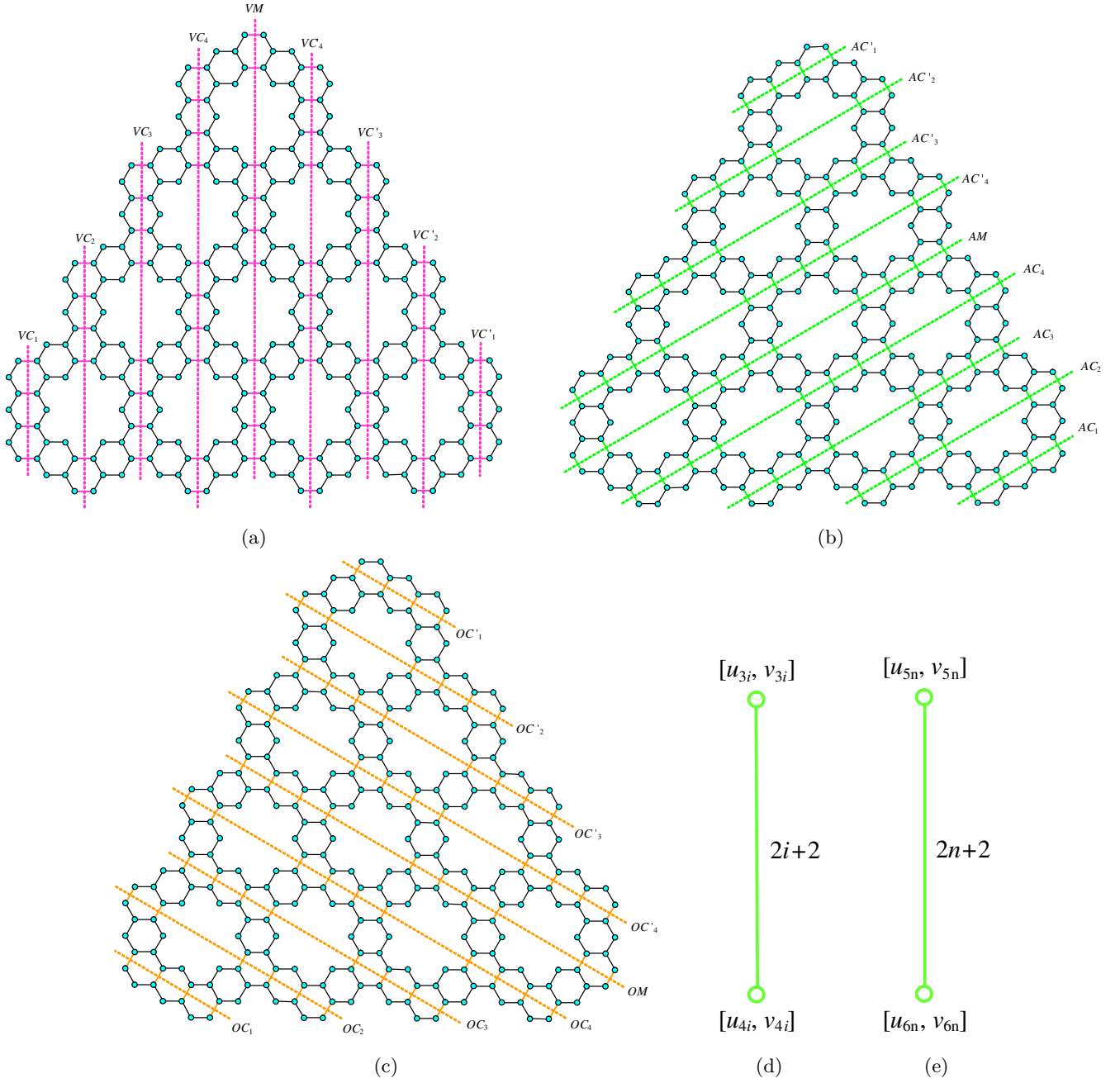
Figure 3: Θ-classes of kekulene structure (a) Vertical Cut; (b) Acute cut; (c) Obtuse cut; (d) Quotient graph of vertical, acute and obtuse cuts for the range $1 \leq i \leq n$; (e) Quotient graph for middle cuts

Table 3: Strength-weighted values of quotient graphs of triangular tessellation of kekulene system $TK(n)$

Quotient graph	Vertex weight: w_v	Vertex strength: s_v
G/AZ_i	$u_{1i} = 9i^2 + 15i - 2$	$v_{1i} = 12i^2 + 18i - 4$
$1 \leq i \leq n$	$u_{2i} = |V(G)| - u_{1i} - 2(i+1)$	$v_{2i} = |E(G)| - v_{1i} - 4(i+1)$
G/AC_i	$u_{3i} = (9i^2 + 15i - 10)/2$	$v_{3i} = 6i^2 + 8i - 8$
$1 \leq i \leq n$	$u_{4i} = |V(G)| - u_{3i}$	$v_{4i} = |E(G)| - v_{3i} - 2i - 2$
G/AM	$u_{5n} = |V|/2$	$v_{5n} = (|E| - (2n+2))/2$
	$u_{6n} = u_{5n}$	$v_{6n} = v_{5n}$

$$W(G) = 3\left[\sum_{i=1}^{n}[2(i+1)(u_{1i} + u_{2i}) + 2u_{1i}u_{2i} + 2(i+1)(2(i+1) - 1)] + 2\sum_{i=1}^{n} u_{3i}u_{4i} + u_{5n}u_{6n}\right].$$

$$W_e(G) = 3\left[\sum_{i=1}^{n}[2(i+1)(v_{1i} + v_{2i}) + 2v_{1i}v_{2i} + 2(i+1)(2(i+1) - 1)] + 2\sum_{i=1}^{n} v_{3i}v_{4i} + v_{5n}v_{6n}\right].$$

$$W_{ve}(G) = \frac{3}{2}\left[\sum_{i=1}^{n}[2(i+1)(u_{1i} + u_{2i} + v_{1i} + v_{2i}) + 2(u_{1i}v_{2i} + v_{1i}u_{2i}) + 4(i+1)(2(i+1) - 1)] \right.$$
$$\left. + 2\sum_{i=1}^{n}[u_{3i}v_{4i} + v_{3i}u_{4i}] + u_{5n}v_{6n} + v_{5n}u_{6n}\right].$$

$$Sz_v(G) = 3\left[\sum_{i=1}^{n}\left[2(i+1)[(u_{1i} + 2(i+1) - 1)(u_{2i} + 1) + (u_{2i} + 2(i+1) - 1)(u_{1i} + 1)]\right] \right.$$
$$\left. + 2\sum_{i=1}^{n}[(2i+2)u_{3i}u_{4i}] + (2n+2)u_{5n}u_{6n}\right].$$

$$Sz_e(G) = 3\left[\sum_{i=1}^{n}\left[2(i+1)[(v_{1i} + 2(i+1) - 1)(v_{2i} + 1) + (v_{2i} + 2(i+1) - 1)(v_{1i} + 1)]\right] \right.$$
$$\left. + 2\sum_{i=1}^{n}[(2i+2)v_{3i}v_{4i}] + (2n+2)v_{5n}v_{6n}\right].$$

$$Sz_{ev}(G) = 3\left[\sum_{i=1}^{n}\left[2(i+1)[(u_{1i} + 2(i+1) - 1)(v_{2i} + 1) + (v_{1i} + 2(i+1) - 1)(u_{2i} + 1)\right.\right.$$
$$\left. + (u_{2i} + 2(i+i) - 1)(v_{1i} + 1) + (v_{2i} + 2(i+1) - 1)(u_{1i} + 1)]\right]$$
$$\left. + 2\sum_{i=1}^{n}[(2i+2)(u_{3i}v_{4i} + v_{3i}u_{4i})] + (2n+2)(u_{5n}v_{6n} + v_{5n}u_{6n})\right].$$

$$PI(G) = 3\left[\sum_{i=1}^{n} 2(i+1)[(v_{1i} + 2(i+1) - 1) + (v_{2i} + 1) + (v_{2i} + 2(i+1) - 1) + (v_{1i} + 1)]\right.$$

$$+ 2 \sum_{i=1}^{n} [(2i+2)(v_{3i} + v_{4i})] + (2n+2)(v_{5n} + v_{6n}) \Bigg].$$

$$S(G) = 3 \Bigg[\sum_{i=1}^{n} \Big[2(i+1)[2(u_{1i} + u_{2i} + v_{1i} + v_{2i}) + 4(i+1)] + 2[u_{1i}(2v_{2i} + 2(i+1))$$

$$+ u_{2i}(2v_{1i} + 2(i+1))] + 8(i+1)(2(i+1)-1)] + 2 \sum_{i=1}^{n} [u_{3i}(2v_{4i} + 2i + 2)$$

$$+ u_{4i}(2v_{3i} + 2i + 2)] + u_{5n}(2v_{6n} + 2n + 2) + u_{6n}(2v_{5n} + 2n + 2) \Bigg].$$

$$Gut(G) = 3 \Bigg[\sum_{i=1}^{n} \Big[4(i+1)[2(v_{1i} + v_{2i} + 4(i+1))] + 2(2v_{2i} + 2(i+1))(2v_{1i} + 2(i+1))$$

$$+ 8(i+1)(2(i+1)-1)] + 2 \sum_{i=1}^{n} [(2v_{3i} + 2i + 2)(2v_{4i} + 2i + 2)] + (2v_{5n} + 2n + 2)$$

$$(2v_{6n} + 2n + 2) \Bigg].$$

□

The results of the above theorem are represented in the following Figure 4.
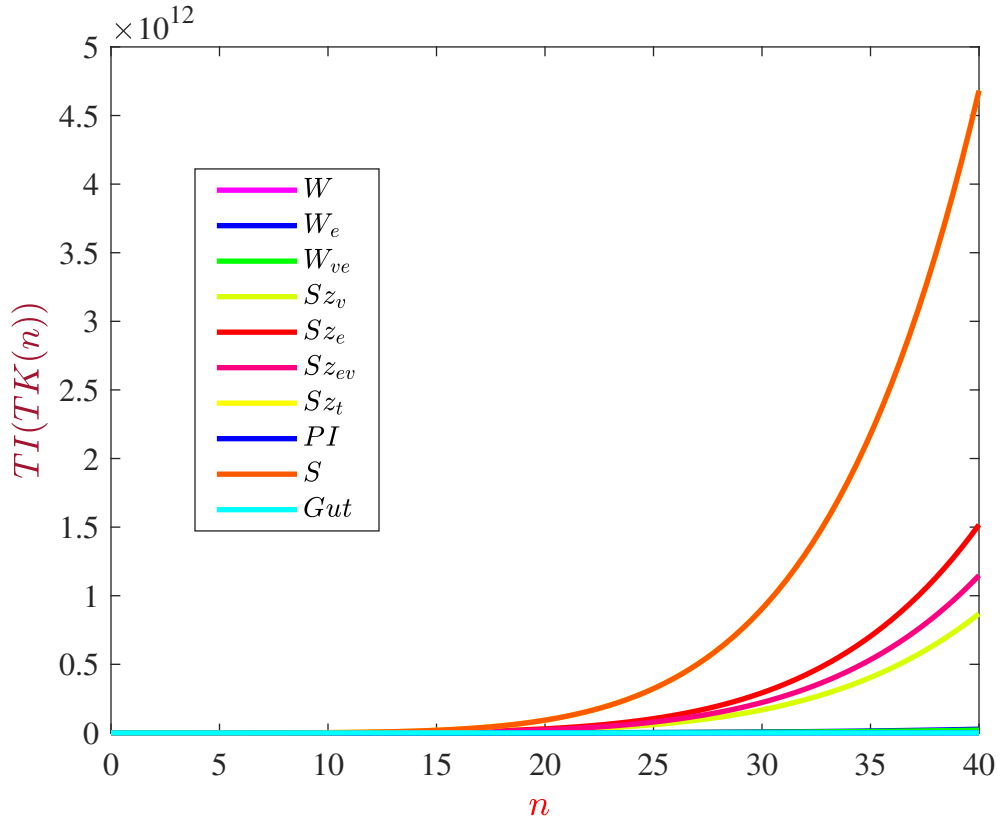

Figure 4: Graphical representation of topological indices of $TK(n)$

Theorem 3. *Let G be a triangular tessellation of kekulene system $TK(n)$. Then,*

(i) $R(G) = (2n^2\left(\sqrt{6}+2\right) + 2n\left(4\sqrt{6}+6.5\right) + 2\sqrt{6}+1)/2.$

(ii) $RR(G) = (18+6\sqrt{6})n^2 + (51+24\sqrt{6})n + 6\sqrt{6}-3.$

(iii) $RRR(G) = (6\sqrt{2}+12)n^2 + (33+24\sqrt{2})n + 6\sqrt{2}-3.$

(iv) $M_1(G) = 66n^2 + 222n + 24.$

(v) $M_2(G) = 90n^2 + 291n + 21.$

(vi) $RM_2(G) = 36n^2 + 111n + 3.$

(vii) $HM(G) = 366n^2 + 1188n + 90.$

(viii) $AZ(G) = \left(7446n^2 + 24759n + 2421\right)/64.$

(ix) $ABC(G) = ((6+4\sqrt{2})n^2 + (27+10\sqrt{2})n + 9 - 2\sqrt{2})/\sqrt{2}.$

(x) $H(G) = \left(44n^2 + 161n + 29\right)/10.$

(xi) $SC(G) = ((4\sqrt{15}+12\sqrt{2})n^2 + (3\sqrt{10}+48\sqrt{2}+10\sqrt{15})n + 3\sqrt{10}+12\sqrt{2}-2\sqrt{15})/2\sqrt{10}.$

(xii) $GA(G) = ((30 + +12\sqrt{6})n^2 + (90+48\sqrt{6})n + 12\sqrt{6})/5.$

(xiii) $ISI(G) = (162n^2 + 543n + 57)/10.$

(xiv) $PM_1(G) = 4^{3n+3} \times 5^{6n^2+24n+6} \times 6^{6n^2+15n-3}.$

(xv) $PM_2(G) = 4^{3n+3} \times 6^{6n^2+24n+6} \times 9^{6n^2+15n-3}.$

The above results are simple along with the values of the following Table 4.

Table 4: The edge partition of triangular tessellation of kekulene system $TK(n)$

S. No	Edge Type	$(d(u), d(v))$	Frequency
1	E_1	(2,2)	$3n+3$
2	E_2	(2,3)	$6n^2 + 24n + 6$
3	E_3	(3,3)	$6n^2 + 15n - 3$

The computed numerical values of various degree-based indices for first 10 dimensions of $TK(n)$ are presented in Table 5 and Table 6. The graphical representation of various degree-based topological indices of triangle kekulene are depicted in Figure 5 and Figure 6.

13

Table 5: Computed numerical values of $R(G)$, $RR(G)$, $RRR(G)$, $M_1(G)$, $M_2(G)$, $RM(G)$, and $HM(G)$ for $G = TK(n)$

n	$R(G)$	$RR(G)$	$RRR(G)$	$M_1(G)$	$M_2(G)$	$RM(G)$	$HM(G)$
1	24	154	93	312	402	150	1644
2	53	362	221	732	963	369	3930
3	92	635	391	1284	1704	660	6948
4	139	974	601	1968	2625	1023	10698
5	196	1378	852	2784	3726	1458	15180
6	261	1848	1145	3732	5007	1965	20394
7	335	2382	1478	4812	6468	2544	26340
8	418	2983	1852	6024	8109	3195	33018
9	510	3648	2267	7368	9930	3918	40428
10	611	4379	2723	8844	11931	4713	48570

Table 6: Computed numerical values of $AZ(G)$, $ABC(G)$, $H(G)$, $SC(G)$, $GA(G)$, and $ISI(G)$ for $G = TK(n)$

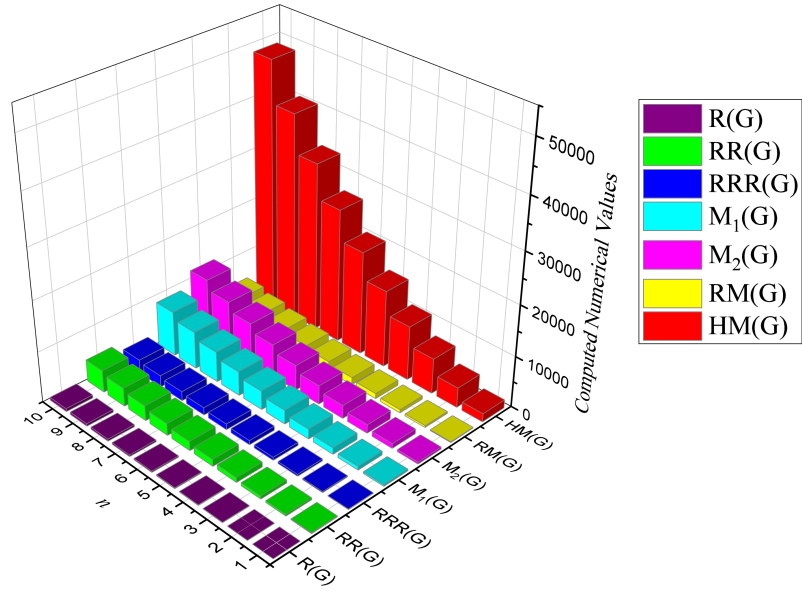| n	$AZ(G)$	$ABC(G)$	$H(G)$	$SC(G)$	$GA(G)$	$ISI(G)$
1	541	42	23	264	59	76
2	1277	83	53	602	136	179
3	2246	132	91	1042	237	314
4	3447	189	138	1585	362	482
5	4881	254	193	2231	510	682
6	6547	327	258	2979	683	915
7	8447	408	331	3830	879	1180
8	10579	497	413	4783	1098	1477
9	12943	594	504	5839	1342	1807
10	15541	700	604	6998	1609	2169

Figure 5: For $G = TK_n$, graphical representation of degree-based indices $R(G)$, $RR(G)$, $RRR(G)$, $M_1(G)$, $M_2(G)$, $RM(G)$, and $HM(G)$
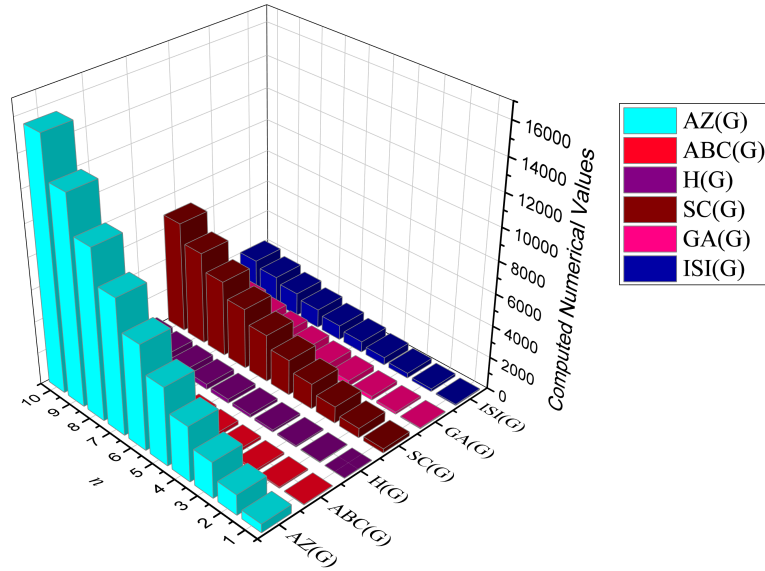

Figure 6: For $G = TK_n$, the graphical representation of degree-based indices $AZ(G)$, $ABC(G)$, $H(G)$, $SC(G)$, $GA(G)$, and $ISI(G)$

Theorem 4. *Let G be a rhombus tessellation of kekulene system $RK(n)$. Then,*

(i) $W(G) = (20493n^5 + 91080n^4 + 93295n^3 + 1800n^2 + 902n - 30)/30.$

(ii) $W_e(G) = (18216n^5 + 71580n^4 + 54460n^3 - 15450n^2 + 4424n - 210)/15.$

(iii) $W_{ve}(G) = (27324n^5 + 114405n^4 + 102310n^3 - 11865n^2 + 3386n - 120)/30.$

(iv) $Sz_v(G) = (19440n^6 + 106362n^5 + 186835n^4 + 103280n^3 - 5335n^2 + 3478n - 60)/15.$

(v) $Sz_e(G) = (11520n^6 + 57264n^5 + 87240n^4 + 30480n^3 - 14100n^2 + 4776n - 180)/5.$

(vi) $Sz_{ev}(G) = (5184n^6 + 27066n^5 + 44405n^4 + 20208n^3 - 4289n^2 + 1422n - 36)/3.$

(vii) $Sz_t(G) = (211680n^6 + 1097628n^5 + 1785210n^4 + 793600n^3 - 181050n^2 + 64052n - 1920)/30.$

(viii) $PI(G) = (8n(252n^3 + 905n^2 + 741n - 134))/3.$

(ix) $S(G) = (54648n^5 + 235290n^4 + 226940n^3 - 6330n^2 + 3652n - 120)/15.$

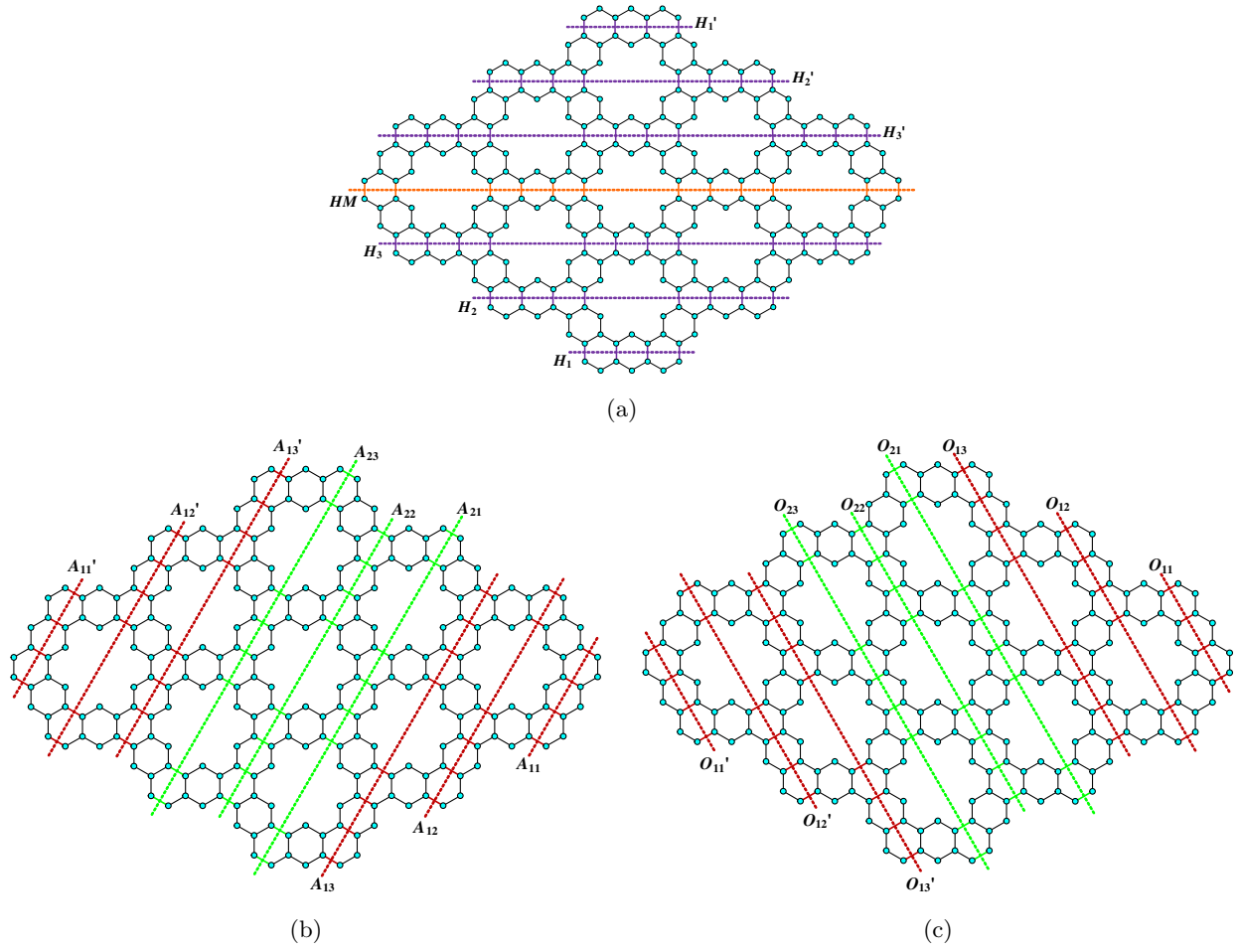(x) $Gut(G) = (72864n^5 + 303600n^4 + 274760n^3 - 21360n^2 + 6856n - 240)/15.$

16

(a)

(b)   (c)

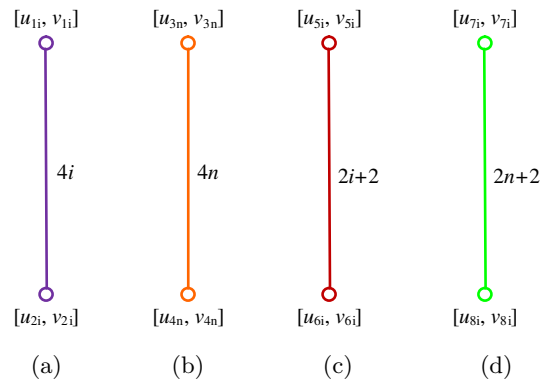Figure 7: Θ-classes of kekulene structure (a) Horizontal cut; (b) Acute Cut ; (c) Obtuse cut

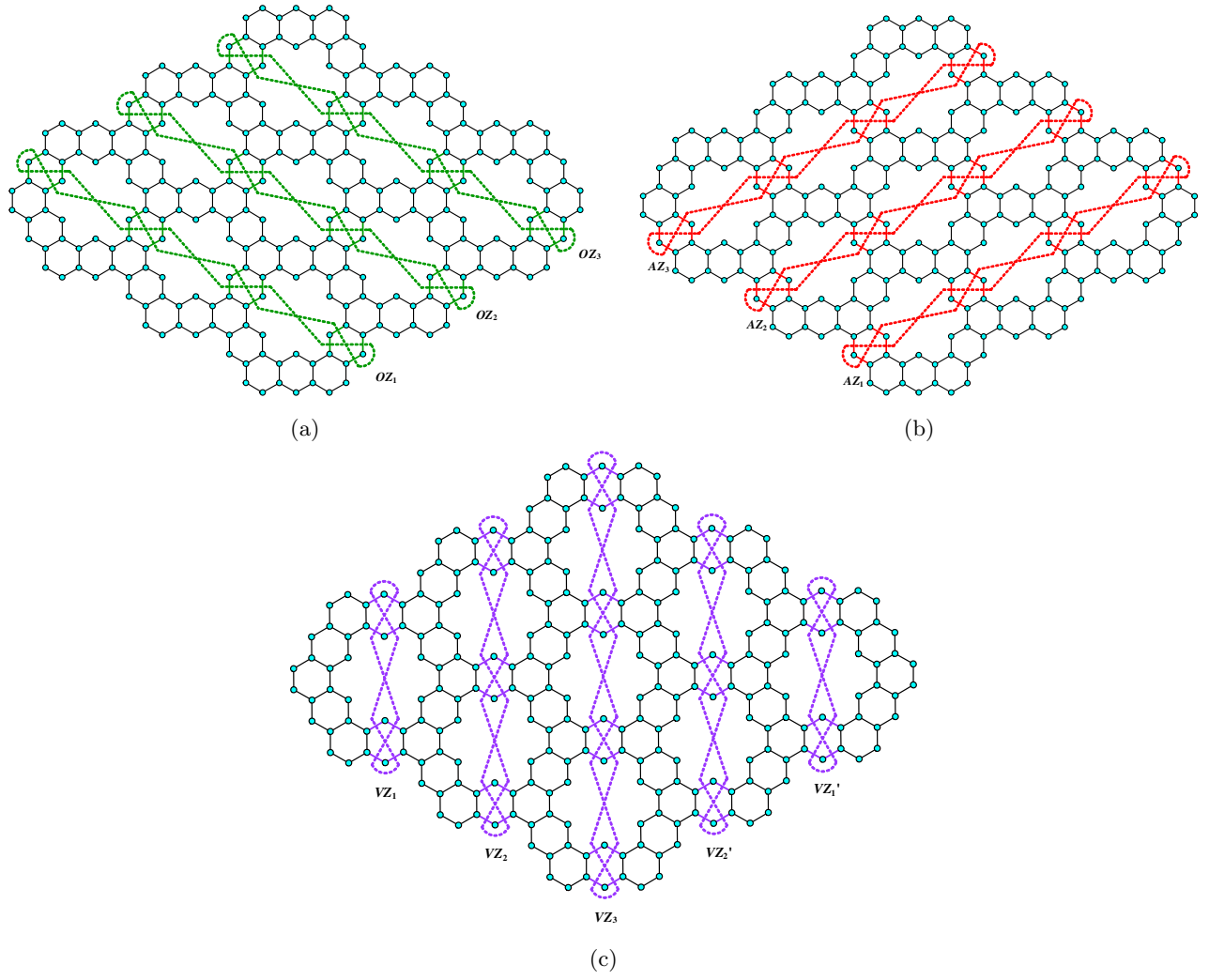Figure 8: Quotient Graph (a) G/H_i; (b) G/HM; (c) G/A_{1i}; (d) G/A_{2i}

Figure 9: Θ^*-classes of kekulene structure (a) Obtuse zigzag; (b) Acute zigzag; (c) Vertical zigzag
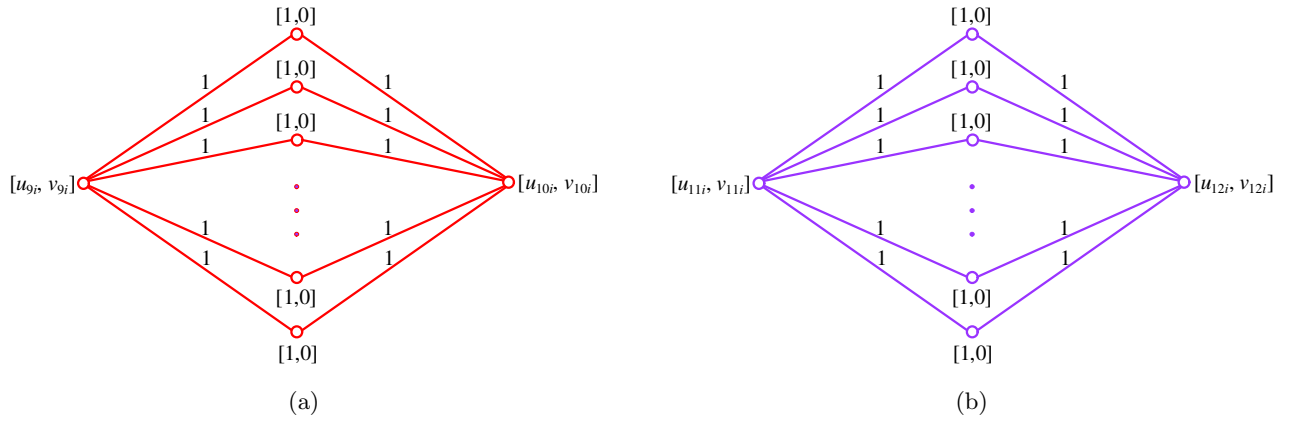

Figure 10: Quotient Graph (a) G/AZ_i; (b) G/VZ_i

18

Table 7: Strength weighted values of rhombus tessellation of kekulene system $RK(n)$

Quotient Graph	Vertex weight : w_v	Vertex strength : s_v
G/H_i $1 \leq i \leq n$	$u_{1i} = 9i^2 - 2i$ $u_{2i} = |V(G)| - u_{1i}$	$v_{1i} = 12i^2 - 6i$ $v_{2i} = |E(G)| - v_{1i} - 4i$
G/HM	$u_{3n} = \frac{1}{2}(|V|)$ $u_{4n} = u_{3n}$	$v_{3n} = \frac{1}{2}(|E| - 4n)$ $v_{4n} = v_{3n}$
G/A_{1i} $1 \leq i \leq n$	$u_{5i} = \frac{1}{2}(9i^2 + 15i - 10)$ $u_{6i} = |V(G)| - u_{5i}$	$v_{5i} = 6i^2 + 8i - 8$ $v_{6i} = |E(G)| - v_{5i} - 2(i+1)$
G/A_{2i} $1 \leq i \leq n$	$u_{7i} = \frac{1}{2}(9n^2 + 15n + 18ni + 16i - 10)$ $u_{8i} = |V(G)| - u_{7i}$	$v_{7i} = 6n^2 + 8n + 12ni + 10i - 8$ $v_{8i} = |E(G)| - v_{7i} - 2(n+1)$
G/AZ_i $1 \leq i \leq n$	$u_{9i} = 18ni + 16i - 2n - 10$ $u_{10i} = |V(G)| - u_{9i} - 2(n+1)$	$v_{9i} = 24ni + 20i - 4n - 14$ $v_{10i} = |E(G)| - b_{9i} - 4(n+1)$
G/VZ_i $1 \leq i \leq n$	$u_{11i} = 9i^2 + 15i - 2$ $u_{12i} = |V(G)| - u_{11i} - 2(i+1)$	$v_{11i} = 12i^2 + 18i - 4$ $v_{12i} = |E(G)| - v_{11i} - 4(i+1)$

Proof. The number of vertices and edges of $RK(n)$ are given respectively by $18n^2 + 32n - 2$ and $24n^2 + 40n - 4$. With this we let $\{H_i : 1 \leq i \leq 3\}$ and HM be the horizontal cuts and horizontal middle cut which are Θ-classes depicted in Figure 7(a), and the cuts $\{H_i : 1 \leq i \leq 3\}$ are symmetrical with $\{H'_i : 1 \leq i \leq 3\}$. The other Θ-classes in $PK(n)$ are $\{A_{1i} : 1 \leq i \leq 3\}$, $\{A'_{1i} : 1 \leq i \leq 3\}$, and $\{A_{2i} : 1 \leq i \leq 3\}$ depicted in Figure 7(b) in which A'_{1i} and A_{1i} cuts results an isomorphic quotient graph, same is depicted in Figure 8(c) along with its strength weighted values. Similarly, it happens for $\{O_{1i} : 1 \leq i \leq 3\}$, $\{O'_{1i} : 1 \leq i \leq 3\}$, and $\{O_{2i} : 1 \leq i \leq 3\}$. See Figure 7(c). The quotient graph of $\{A_{2i} : 1 \leq i \leq 3\}$ and $\{O_{2i} : 1 \leq i \leq 3\}$ are isomorphic and the same is depicted in Figure 8(d). Let $\{OZ_i : 1 \leq i \leq 3\}$, $\{AZ_i : 1 \leq i \leq 3\}$, and $\{VZ_i : 1 \leq i \leq 3\}$ be the obtuse zigzag and acute zigzag and vertical zigzag cuts respectively depicted in Figure 9(a), 9(b), and 9(c). The quotient graph of obtuse zigzag and acute zigzag are isomorphic and the same is depicted in Figure 10(a); and the quotient graph for vertical zigzag is depicted in Figure 10(b) and corresponding strength-weigthted values are given in the Table 7.

$$W(G) = 2\sum_{i=1}^{n} u_{1i}u_{2i} + u_{3n}u_{4n} + 4\sum_{i=1}^{n} u_{5i}u_{6i} + 2\sum_{i=1}^{n} u_{7i}u_{8i}$$

$$+ 2\sum_{i=1}^{n}[2(n+1)(u_{9i} + u_{10i}) + 2u_{9i}u_{10i} + 2(n+1)(2(n+1) - 1)]$$

$$+ \sum_{i=1}^{n}[2(i+1)(u_{11i} + u_{12i}) + 2u_{11i}u_{12i} + 2(i+1)(2(i+1) - 1)]$$

$$+ \sum_{i=1}^{n-1}[2(i+1)(u_{11i} + u_{12i}) + 2u_{11i}u_{12i} + 2(i+1)(2(i+1) - 1)].$$

$$W_e(G) = 2\sum_{i=1}^{n} v_{1i}v_{2i} + v_{3n}v_{4n} + 4\sum_{i=1}^{n} v_{5i}v_{6i} + 2\sum_{i=1}^{n} v_{7i}v_{8i}$$

$$+ 2\sum_{i=1}^{n}[2(n+1)(v_{9i} + v_{10i}) + 2v_{9i}v_{10i} + 2(n+1)(2(n+1) - 1)]$$

$$+ \sum_{i=1}^{n}[2(i+1)(v_{11i} + v_{12i}) + 2v_{11i}v_{12i} + 2(i+1)(2(i+1) - 1)]$$

$$+ \sum_{i=1}^{n-1}[2(i+1)(v_{11i} + v_{12i}) + 2v_{11i}v_{12i} + 2(i+1)(2(i+1) - 1)].$$

$$W_{ve}(G) = \frac{1}{2}\left[2\sum_{i=1}^{n}[u_{1i}v_{2i} + u_{2i}v_{1i}] + [u_{3n}v_{4n} + u_{4n}v_{3n}] + 4\sum_{i=1}^{n}[u_{5i}v_{6i} + u_{6i}v_{5i}] + 2\sum_{i=1}^{n}[u_{7i}v_{8i} + u_{8i}v_{7i}]\right.$$

$$+ 2\sum_{i=1}^{n} 2(n+1)(u_{9i} + u_{10i} + v_{9i} + v_{10i}) + 2(u_{9i}v_{10i} + u_{10i}v_{9i}) + 4(n+1)(2(n+1) - 1)$$

$$+ \sum_{i=1}^{n} 2(i+1)(u_{11i} + u_{12i} + v_{11i} + v_{12i}) + 2(u_{11i}v_{12i} + u_{12i}v_{11i}) + 4(i+1)(2(i+1) - 1)$$

$$\left.+ \sum_{i=1}^{n-1} 2(i+1)(u_{11i} + u_{12i} + v_{11i} + v_{12i}) + 2(u_{11i}v_{12i} + u_{12i}v_{11i}) + 4(i+1)(2(i+1) - 1)\right].$$

$$Sz_v(G) = 2\sum_{i=1}^{n} 4iu_{1i}u_{2i} + 4nu_{3n}u_{4n} + 4\sum_{i=1}^{n} 2(i+1)u_{5i}u_{6i} + 2\sum_{i=1}^{n} 2(n+1)u_{7i}u_{8i}$$

$$+ 2\sum_{i=1}^{n} 2(n+1)[(u_{9i} + 2(n+1) - 1)(u_{10i} + 1) + (u_{10i} + 2(n+1) - 1)(u_{9i} + 1)]$$

$$+ \sum_{i=1}^{n} 2(i+1)[(u_{11i} + 2(i+1) - 1)(u_{12i} + 1) + (u_{12i} + 2(i+1) - 1)(u_{11i} + 1)]$$

$$+ \sum_{i=1}^{n-1} 2(i+1)[(u_{11i} + 2(i+1) - 1)(u_{12i} + 1) + (u_{12i} + 2(i+1) - 1)(u_{11i} + 1)].$$

$$Sz_e(G) = 2\sum_{i=1}^{n} 4iv_{1i}v_{2i} + 4nv_{3n}v_{4n} + 4\sum_{i=1}^{n} 2(i+1)v_{5i}v_{6i} + 2\sum_{i=1}^{n} 2(n+1)v_{7i}v_{8i}$$

$$+ 2\sum_{i=1}^{n} 2(n+1)[(v_{9i} + 2(n+1) - 1)(v_{10i} + 1) + (v_{10i} + 2(n+1) - 1)(v_{9i} + 1)]$$

$$+ \sum_{i=1}^{n} 2(i+1)[(v_{11i} + 2(i+1) - 1)(v_{12i} + 1) + (v_{12i} + 2(i+1) - 1)(v_{11i} + 1)]$$

$$+ \sum_{i=1}^{n-1} 2(i+1)[(v_{11i} + 2(i+1) - 1)(v_{12i} + 1) + (v_{12i} + 2(i+1) - 1)(v_{11i} + 1)].$$

$$Sz_{ev}(G) = \frac{1}{2}\left[2\sum_{i=1}^{n} 4i[u_{1i}v_{2i} + u_{2i}v_{1i}] + 4n[u_{3n}v_{4n} + u_{4n}v_{3n}] + 4\sum_{i=1}^{n} 2(i+1)[u_{5i}v_{6i} + u_{6i}v_{5i}]\right.$$

20

$$+ 2\sum_{i=1}^{n} 2(n+1)[u_{7i}v_{8i} + u_{8i}v_{7i}] + 2\sum_{i=1}^{n} 2(n+1)[(u_{9i} + 2(n+1) - 1)(v_{10i} + 1)$$

$$+ (v_{9i} + 2(n+1) - 1)(u_{10i} + 1) + (u_{10i} + 2(n+1) - 1)(v_{9i} + 1)$$

$$+ (v_{10i} + 2(n+1) - 1)(u_{9i} + 1)] + \sum_{i=1}^{n} 2(i+1)[(u_{11i} + 2(i+1) - 1)(v_{12i} + 1)$$

$$+ (v_{11i} + 2(i+1) - 1)(u_{12i} + 1) + (u_{12i} + 2(i+1) - 1)(v_{11i} + 1)$$

$$+ (v_{12i} + 2(i+1) - 1)(u_{11i} + 1)] + \sum_{i=1}^{n-1} 2(i+1)[(u_{11i} + 2(i+1) - 1)(v_{12i} + 1)$$

$$+ (v_{11i} + 2(i+1) - 1)(u_{12i} + 1) + (u_{12i} + 2(i+1) - 1)(v_{11i} + 1)$$

$$\left. + (v_{12i} + 2(i+1) - 1)(u_{11i} + 1)] \right]$$

$$PI(G) = 2\sum_{i=1}^{n} 4i(v_{1i} + v_{2i}) + 4n(v_{3n} + v_{4n}) + 4\sum_{i=1}^{n} 2(i+1)(v_{5i} + v_{6i}) + 2\sum_{i=1}^{n} 2(n+1)(v_{7i} + v_{8i})$$

$$+ 2\sum_{i=1}^{n} 2(n+1)[(v_{9i} + 2(n+1) - 1) + (v_{10i} + 1) + (v_{10i} + 2(n+1) - 1) + (v_{9i} + 1)]$$

$$+ \sum_{i=1}^{n} 2(i+1)[(v_{11i} + 2(i+1) - 1) + (v_{12i} + 1) + (v_{12i} + 2(i+1) - 1) + (v_{11i} + 1)]$$

$$+ \sum_{i=1}^{n-1} 2(i+1)[(v_{11i} + 2(i+1) - 1) + (v_{12i} + 1) + (v_{12i} + 2(i+1) - 1) + (v_{11i} + 1)].$$

$$S(G) = 2\sum_{i=1}^{n} [u_{1i}(2v_{2i} + 4i) + u_{2i}(2v_{1i} + 4i)] + [u_{3n}(2v_{4n} + 4n) + u_{4n}(2v_{3n} + 4n)]$$

$$+ 4\sum_{i=1}^{n} [u_{5i}(2v_{6i} + 2i + 2) + u_{6i}(2v_{5i} + 2i + 2)] + 2\sum_{i=1}^{n} [u_{7i}(2v_{8i} + 2n + 2)$$

$$+ u_{8i}(2v_{7i} + 2n + 2)] + 2\sum_{i=1}^{n} 2(n+1)[2(u_{9i} + u_{10i} + v_{9i} + v_{10i}) + 4(n+1)]$$

$$+ 2[u_{9i}(2v_{10i} + 2(n+1)) + u_{10i}(2v_{9i} + 2(n+1))] + 8(n+1)(2(n+1) - 1)$$

$$+ \sum_{i=1}^{n} 2(i+1)[2(u_{11i} + u_{12i} + v_{11i} + v_{12i}) + 4(i+1)] + 2[u_{11i}(2v_{12i} + 2(i+1))$$

$$+ u_{12i}(2v_{11i} + 2(i+1))] + 8(i+1)(2(i+1) - 1)$$

$$+ \sum_{i=1}^{n-1} 2(i+1)[2(u_{11i} + u_{12i} + v_{11i} + v_{12i}) + 4(i+1)] + 2[u_{11i}(2v_{12i} + 2(i+1))$$

$$+ u_{12i}(2v_{11i} + 2(i+1))] + 8(i+1)(2(i+1) - 1).$$

$$Gut(G) = 2\sum_{i=1}^{n} [(2v_{2i} + 4i)(2v_{1i} + 4i)] + [(2v_{4n} + 4n)(2v_{3n} + 4n)]$$

$$+ 4 \sum_{i=1}^{n} [(2v_{6i} + 2i + 2)(2v_{5i} + 2i + 2)] + 2 \sum_{i=1}^{n} [(2v_{8i} + 2n + 2)(2v_{7i} + 2n + 2)]$$

$$+ 2 \sum_{i=1}^{n} 4(n + 1)[2(v_{9i} + v_{10i} + 4(n + 1))] + 2(2v_{9i} + 2(n + 1))(2v_{10i} + 2(n + 1))$$

$$+ 8(n + 1)(2(n + 1) - 1) + \sum_{i=1}^{n} 4(i + 1)[2(v_{11i} + v_{12i} + 4(i + 1))]$$

$$+ 2(2v_{11i} + 2(i + 1))(2v_{12i} + 2(i + 1)) + 8(i + 1)(2(i + 1) - 1)$$

$$+ \sum_{i=1}^{n-1} 4(i + 1)[2(v_{11i} + v_{12i} + 4(i + 1))] + 2(2v_{11i} + 2(i + 1))(2v_{12i} + 2(i + 1))$$

$$+ 8(i + 1)(2(i + 1) - 1).$$

$\square$

The results of the above theorem are represented in the following Figure 11.
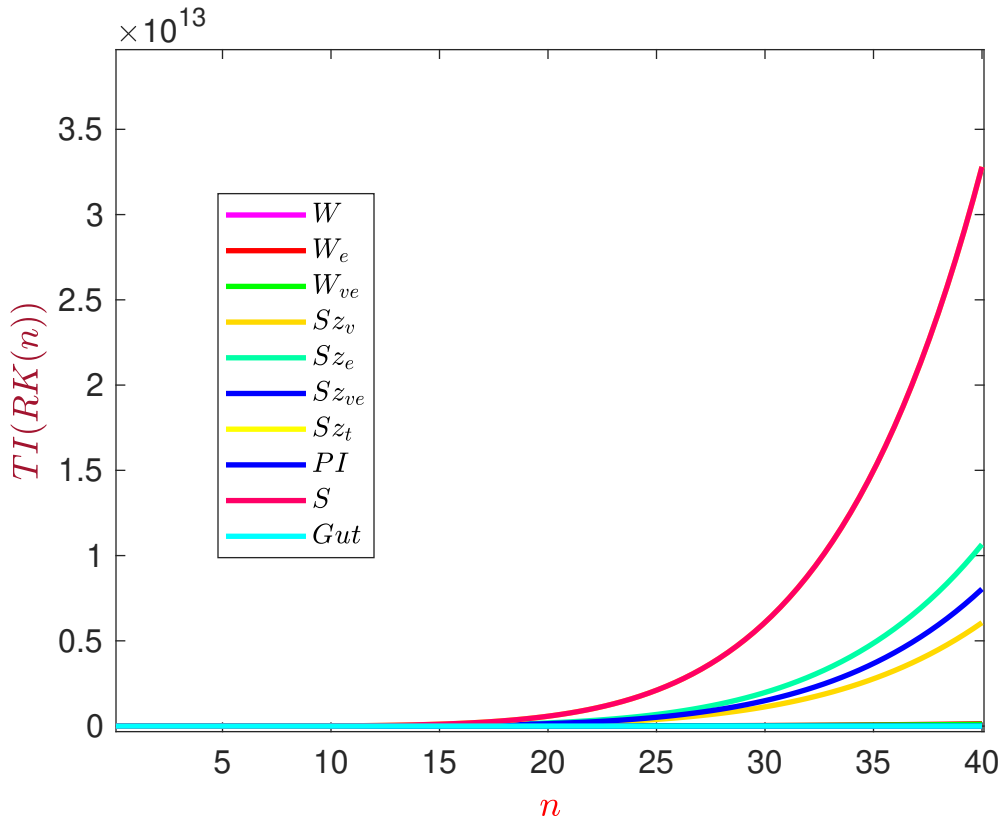

Figure 11: Graphical representation of various distance based topological indices of $RK(n)$

Theorem 5. *Let G be a rhombus tessellation of kekulene system $RK(n)$. Then,*

(i) $R(G) = (4 + 2\sqrt{6})n^2 + (6 + 4\sqrt{6})n - 1.$

(ii) $RR(G) = (36 + 12\sqrt{6})n^2 + (44n + 24\sqrt{6})n - 14.$

(iii) $RRR(G) = (24 + 12\sqrt{2})n^2 + (28 + 24\sqrt{2})n - 10.$

(iv) $M_1(G) = 132n^2 + 208n - 28.$

(v) $M_2(G) = 180n^2 + 268n - 46.$

(vi) $RM_2(G) = 72n^2 + 100n - 22.$

(vii) $HM(G) = 732n^2 + 1096n - 184.$

(viii) $AZ(G) = \left(7446n^2 + 11542n - 1675\right)/32.$

(ix) $ABC(G) = (8 + 6\sqrt{2})n^2 + (8 + 14\sqrt{2})n - 4.$

(x) $H(G) = \left(44n^2 + 78n - 5\right)/5.$

(xi) $SC(G) = \left((12 + 2\sqrt{30})n^2 + (24 + 2\sqrt{30} + 2\sqrt{5})n + \sqrt{5} - \sqrt{30}\right)/\sqrt{5}.$

(xii) $GA(G) = ((60 + 24\sqrt{6})n^2 + (80 + 48\sqrt{6})n - 20)/5.$

(xiii) $ISI(G) = (162n^2 + 254n - 35)/5.$

(xiv) $PM_1(G) = 4^{4n+2} \times 5^{12n^2+24n} \times 6^{12n^2+12n-6}.$

(xv) $PM_2(G) = 4^{4n+2} \times 6^{12n^2+24n} \times 9^{12n^2+12n-6}.$

The proof of the above theorem is simple in line with the values of Table 8.

Table 8: The edge partition of rhombus tessellation of kekulene system $RK(n)$

S. No	Edge Type	$(d(u), d(v))$	Frequency
1	E_1	(2,2)	$4n + 2$
2	E_2	(2,3)	$12n^2 + 24n$
3	E_3	(3,3)	$12n^2 + 12n - 6$

The computed numerical values of various degree-based indices for first 10 dimensions of $RK(n)$ are presented in Table 9 and Table 10. The graphical representation of these degree-based indices are depicted in Figure 12 and Figure 13.

Table 9: Computed numerical value for degree-based indices $R(G)$, $RR(G)$, $RRR(G)$, $M_1(G)$, $M_2(G)$, $RM(G)$, and $HM(G)$ for $G = RK(n)$

n	$R(G)$	$RR(G)$	$RRR(G)$	$M_1(G)$	$M_2(G)$	$RM_2(G)$	$HM(G)$
1	24	154	93	312	402	150	1644
2	66	541	278	916	1210	466	4936
3	126	1147	545	1784	2378	926	9692
4	205	1971	893	2916	3906	1530	15912
5	300	3015	1324	4312	5794	2278	23596
6	414	4277	1837	5972	8042	3170	32744
7	546	5758	2431	7896	10650	4206	43356
8	695	7458	3108	10084	13618	5386	55432
9	862	9376	3866	12536	16946	6710	68972
10	1047	11513	4706	15252	20634	8178	83976

Table 10: Computed numerical value for degree-based indices $AZ(G)$, $ABC(G)$, $H(G)$, $SC(G)$, $GA(G)$, and $ISI(G)$ for $G = RK(n)$

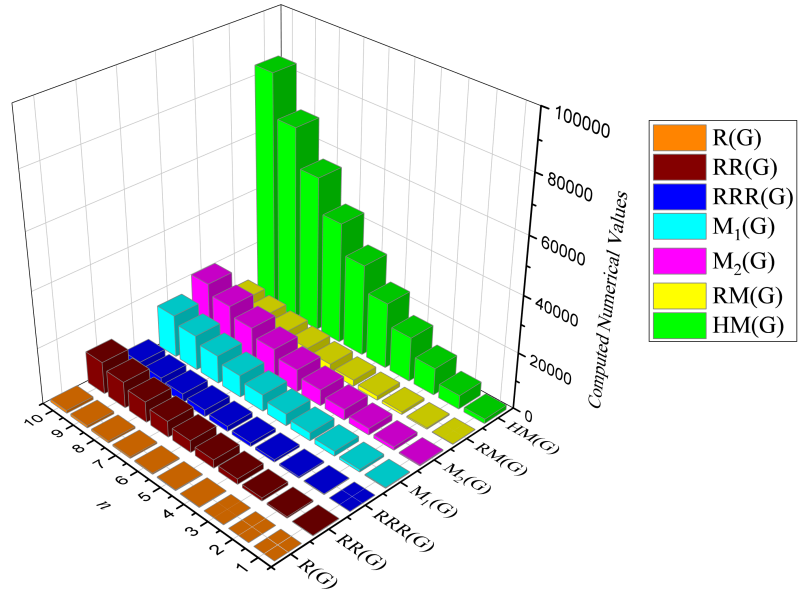| n	$AZ(G)$	$ABC(G)$	$H(G)$	$SC(G)$	$GA(G)$	$ISI(G)$
1	541	40	23	26	59	76
2	1600	118	65	75	170	224
3	3124	228	125	144	328	437
4	5113	371	202	233	534	715
5	7568	547	297	343	788	1057
6	10489	756	409	474	1088	1464
7	13874	998	539	625	1437	1936
8	17725	1273	687	797	1833	2473
9	22042	1581	852	989	2276	3075
10	26823	1923	1035	1201	2767	3741

Figure 12: For $G = RK(n)$, the graphical representation of degree-based indices $R(G)$, $RR(G)$, $RRR(G)$, $M_1(G)$, $M_2(G)$, $RM(G)$, and $HM(G)$
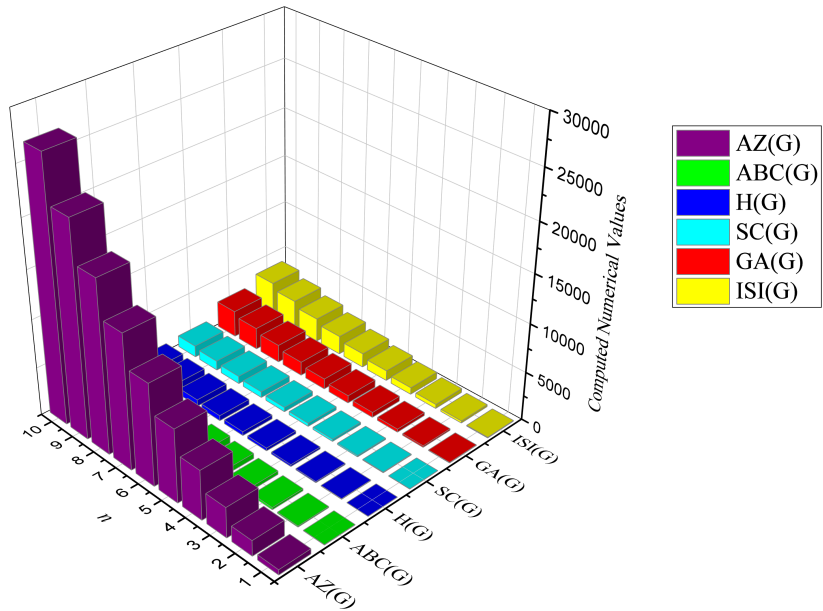

Figure 13: For $G = RK(n)$, the graphical representation of degree-based indices $AZ(G)$, $ABC(G)$, $H(G)$, $SC(G)$, $GA(G)$, and $ISI(G)$

4   Conclusion

We have given the topological indices of two classes of massive polycyclic aromatic compounds made using armchair kekulene systems in triangular and rhombus layouts. The strength-weighted graph strategy is used to compute analytical expressions for the topological indices of these tessellations. The calculations are carried out in MATLAB, and the results are validated in newGRAPH. The results obtained here could potentially provide a vital tool for realizing the importance of these large-sized aromatic compounds when combined with quantum chemical descriptors in various fields such as material science, predictive toxicology, drug discovery, and so on, because the molecular descriptors describe the topological connectivity properties of these compounds.

References

[1] Hussein I. Abdel-Shafy and Mona S.M. Mansour. A review on polycyclic aromatic hydrocarbons: Source, environmental impact, effect on human health and remediation. *Egyptian Journal of Petroleum*, 25:107–123, 3 2016.

[2] Michael O. Albertson. The irregularity of a graph. *Ars Combinatoria*, 46:219–225, 1997.

[3] M. Arejdal. Prediction of the magnetocaloric behaviors of the kekulene structure for the magnetic refrigeration. *Results in Physics*, 18:103342, 9 2020.

[4] Micheal Arockiaraj, Joseph Clement, and Krishnan Balasubramanian. Topological indices and their applications to circumcised donut benzenoid systems, kekulenes and drugs. *Polycyclic Aromatic Compounds*, 40:280–303, 3 2020.

[5] Micheal Arockiaraj, Jia-Bao Liu, M. Arulperumjothi, and S. Prabhu. On certain topological indices of three-layered single-walled titania nanosheets. *Combinatorial Chemistry High Throughput Screening*, 25:483–495, 3 2022.

[6] Micheal Arockiaraj, S. Prabhu, M. Arulperumjothi, S. Ruth Julie Kavitha, and Krishnan Balasubramanian. Topological characterization of hexagonal and rectangular tessellations of kekulenes as traps for toxic heavy metal ions. *Theoretical Chemistry Accounts*, 140:43, 4 2021.

[7] Krishnan Balasubramanian. Combinatorial enumeration of isomers of superaromatic polysubstituted cycloarenes and coronoid hydrocarbons with applications to nmr. *The Journal of Physical Chemistry A*, 122:8243–8257, 10 2018.

[8] S. C. Basak, D. Mills, and M. M. Mumtaz. A quantitative structure–activity relationship (qsar) study of dermal absorption using theoretical molecular descriptors. *SAR and QSAR in Environmental Research*, 18:45–55, 1 2007.

[9] Uliana Beser, Marcel Kastler, Ali Maghsoumi, Manfred Wagner, Chiara Castiglioni, Matteo Tommasini, Akimitsu Narita, Xinliang Feng, and Klaus Müllen. A c216-nanographene molecule with defined cavity as extended coronoid. *Journal of the American Chemical Society*, 138:4322–4325, 4 2016.

[10] Béla Bollobás and Paul Erdös. Graphs of extremal weights. *Ars Combinatoria*, 50:225–233, 1998.

[11] Jonathan C. Buttrick and Benjamin T. King. Kekulenes, cycloarenes, and heterocycloarenes: addressing electronic structure and aromaticity through experiments and calculations. *Chemical Society Reviews*, 46:7–20, 2017.

[12] Yu-Ming Chu, K. Julietraja, P. Venugopal, Muhammad Kamran Siddiqui, and Savari Prabhu. Degree- and irregularity-based molecular descriptors for benzenoid systems. *The European Physical Journal Plus*, 136:78, 1 2021.

[13] François Diederich and Heinz A. Staab. Benzenoid versus annulenoid aromaticity: Synthesis and properties of kekulene. *Angewandte Chemie International Edition in English*, 17:372–374, 5 1978.

[14] Ernesto Estrada. The abc matrix. *Journal of Mathematical Chemistry*, 55:1021–1033, 4 2017.

[15] Ernesto Estrada, Luis A. Torres, Lissette Rodríguez, and Ivan Gutman. An atom-bond connectivity index : Modelling the enthalpy of formation of alkanes. *Indian journal of chemistry. Sect. A: Inorganic, physical, theoretical & analytical*, 37:849–855, 1998.

[16] Siemion Fajtlowicz. On conjectures of graffiti-ii. *Congressus Numerantium*, 60:187–197, 1987.

[17] O. Favaron, M. Mahéo, and J.-F. Saclé. Some eigenvalue properties in graphs (conjectures of graffiti — ii). *Discrete Mathematics*, 111:197–220, 2 1993.

[18] Boris Furtula, Ante Graovac, and Damir Vukičević. Augmented zagreb index. *Journal of Mathematical Chemistry*, 48:370–380, 8 2010.

[19] Boris Furtula, Ivan Gutman, and Matthias Dehmer. On structure-sensitivity of degree-based topological indices. *Applied Mathematics and Computation*, 219:8973–8978, 5 2013.

[20] Boris Furtula, Ivan Gutman, and Süleyman Ediz. On difference of zagreb indices. *Discrete Applied Mathematics*, 178:83–88, 12 2014.

[21] I. Gutman and N. Trinajstić. Graph theory and molecular orbitals. total -electron energy of alternant hydrocarbons. *Chemical Physics Letters*, 17:535–538, 12 1972.

[22] Ivan Gutman and Jelena Tosovic. Testing the quality of molecular structure descriptors. vertex-degree-based topological indices. *Journal of the Serbian Chemical Society*, 78:805–810, 2013.

[23] Balázs Hajgató and Koichi Ohno. Novel series of giant polycyclic aromatic hydrocarbons: electronic structure and aromaticity. *Chemical Physics Letters*, 385:512–518, 2 2004.

[24] Jeremy Hieulle, Eduard Carbonell-Sanromà, Manuel Vilas-Varela, Aran Garcia-Lekue, Enrique Guitián, Diego Peña, and Jose Ignacio Pascual. On-surface route for producing planar nanographenes with azulene moieties. *Nano Letters*, 18:418–423, 1 2018.

[25] Jun ichi Aihara. Graph theory of ring-current diamagnetism. *Bulletin of the Chemical Society of Japan*, 91:274–303, 2 2018.

[26] Jun ichi Aihara and Masakazu Makino. Constrained clar formulas of coronoid hydrocarbons. *The Journal of Physical Chemistry A*, 118:1258–1266, 2 2014.

[27] Jun ichi Aihara, Masakazu Makino, Toshimasa Ishida, and Jerry R. Dias. Analytical study of super-aromaticity in cycloarenes and related coronoid hydrocarbons. *The Journal of Physical Chemistry A*, 117:4688–4697, 6 2013.

[28] Li Ji, Yan Shu, Wu Wenxiang, Li Lingxu, Li Hongda, and Hashem Soleymani. Potential application of kekulene nanoring in the li-ion batteries: Dft studies. *Computational and Theoretical Chemistry*, 1181:112796, 7 2020.

[29] Haijun Jiao and Paul von Ragué Schleyer. Is kekulene really superaromatic? *Angewandte Chemie International Edition in English*, 35:2383–2386, 11 1996.

[30] K. Julietraja, P. Venugopal, S. Prabhu, A.K. Arulmozhi, and M.K. Siddiqui. Structural analysis of three types of pahs using entropy measures. *Polycyclic Aromatic Compounds*, 2021.

[31] K. Julietraja, P. Venugopal, S. Prabhu, S. Deepa, and Muhammad Kamran Siddiqui. Molecular structural descriptors of donut benzenoid systems. *Polycyclic Aromatic Compounds*, 0:1–27, 2021.

[32] K. Julietraja, P. Venugopal, S. Prabhu, and Jia Bao Liu. M-polynomial and degree-based molecular descriptors of certain classes of benzenoid systems. *Polycyclic Aromatic Compounds*, 0:1–30, 2020.

[33] Padmakar Khadikar, Sneha Karmarkar, Vijay Agrawal, Jyoti Singh, Anjali Shrivastava, Istvan Lukovits, and Mircea Diudea. Szeged index - applications for drug modeling. *Letters in Drug Design Discovery*, 2:606–624, 12 2005.

[34] Sandi Klavzar, Ivan Gutman, and Bojan Mohar. Labeling of benzenoid systems which reflects the vertex-distance relations. *Journal of Chemical Information and Computer Sciences*, 35:590–593, 5 1995.

[35] Sandi Klavžar. On the canonical metric representation, average distance, and partial hamming graphs. *European Journal of Combinatorics*, 27:68–73, 1 2006.

[36] Sandi Klavžar and M.J. Nadjafi-Arani. Wiener index in weighted graphs via unification of θ^* -classes. *European Journal of Combinatorics*, 36:71–76, 2 2014.

[37] Chunchen Liu, Yong Ni, Xuefeng Lu, Guangwu Li, and Jishan Wu. Global aromaticity in macrocyclic polyradicaloids: Hückel's rule or baird's rule? *Accounts of Chemical Research*, 52:2309–2321, 8 2019.

[38] Chunchen Liu, María Eugenia Sandoval-Salinas, Yongseok Hong, Tullimilli Y. Gopalakrishna, Hoa Phan, Naoki Aratani, Tun Seng Herng, Jun Ding, Hiroko Yamada, Dongho Kim, David Casanova, and Jishan Wu. Macrocyclic polyradicaloids with unusual super-ring structure and global aromaticity. *Chem*, 4:1586–1595, 7 2018.

[39] Jia-Bao Liu, Micheal Arockiaraj, M Arulperumjothi, and Savari Prabhu. Distance based and bond additive topological indices of certain repurposed antiviral drug compounds tested for treating covid-19. *International Journal of Quantum Chemistry*, 121, 5 2021.

[40] Kian Ping Loh, Shi Wun Tong, and Jishan Wu. Graphene and graphene-like molecules: Prospects in solar cells. *Journal of the American Chemical Society*, 138:1095–1102, 2 2016.

[41] Fernando C.G. Manso, Hélio Scatena, Roy E. Bruns, Adley F. Rubira, and Edvani C. Muniz. Development of a new topological index for the prediction of normal boiling point temperatures of hydrocarbons: The fi index. *Journal of Molecular Liquids*, 165:125–132, 1 2012.

[42] Jamson Masih, Raj Singhvi, Krishan Kumar, V.K. Jain, and Ajay Taneja. Seasonal variation and sources of polycyclic aromatic hydrocarbons (pahs) in indoor and outdoor air in a semi arid tract of northern india. *Aerosol and Air Quality Research*, 12:515–525, 2012.

[43] Charles A. Menzie, Bonnie B. Potocki, and Joseph Santodonato. Exposure to carcinogenic pahs in the environment. *Environmental Science Technology*, 26:1278–1284, 7 1992.

[44] Hirokazu Miyoshi, Shunpei Nobusue, Akihiro Shimizu, and Yoshito Tobe. Non-alternant non-benzenoid kekulenes: the birth of a new kekulene family. *Chemical Society Reviews*, 44:6560–6577, 2015.

[45] Sonja Nikolic, Goran Kovaević, Ante Milicevic, and Nenad Trinajstic. The zagreb indices 30 years after. *Croatica Chemica Acta*, 76:113–124, 2003.

[46] Iago Pozo, Zsolt Majzik, Niko Pavliček, Manuel Melle-Franco, Enrique Guitián, Diego Peña, Leo Gross, and Dolores Pérez. Revisiting kekulene: Synthesis and single-molecule imaging. *Journal of the American Chemical Society*, 141:15488–15493, 10 2019.

[47] S. Prabhu, G. Murugan, Micheal Arockiaraj, M. Arulperumjothi, and V. Manimozhi. Molecular topological characterization of three classes of polycyclic aromatic hydrocarbons. *Journal of Molecular Structure*, 1229:129501, 4 2021.

[48] S. Prabhu, G. Murugan, Michael Cary, M. Arulperumjothi, and Jia-Bao Liu. On certain distance and degree based topological indices of zeolite lta frameworks. *Materials Research Express*, 7:055006, 5 2020.

[49] S. Prabhu, G. Murugan, S. Kulandai Therese, M. Arulperumjothi, and Muhammad Kamran Siddiqui. Molecular structural characterization of cycloparaphenylene and its variants. *Polycyclic Aromatic Compounds*, pages 1–17, 7 2021.

[50] S. Prabhu, Y. Sherlin Nisha, M. Arulperumjothi, D. Sagaya Rani Jeba, and V. Manimozhi. On detour index of cycloparaphenylene and polyphenylene molecular structures. *Scientific Reports*, 11:15264, 12 2021.

[51] M. Radhakrishnan, Savari Prabhu, Micheal Arockiaraj, and M. Arulperumjothi. Molecular structural characterization of superphenalene and supertriphenylene. *International Journal of Quantum Chemistry*, 122:1–18, 2022.

[52] Milan Randic. Characterization of molecular branching. *Journal of the American Chemical Society*, 97:6609–6615, 11 1975.

[53] M. Randići. On history of the randić index and emerging hostility toward chemical graph theory. *MATCH Communications in Mathematical and in Computer Chemistry*, 59:5–124, 2008.

[54] Milan Randić. Aromaticity of polycyclic conjugated hydrocarbons. *Chemical Reviews*, 103:3449–3606, 9 2003.

[55] Alex W. Robertson, Gun-Do Lee, Kuang He, Chuncheng Gong, Qu Chen, Euijoon Yoon, Angus I. Kirkland, and Jamie H. Warner. Atomic structure of graphene subnanometer pores. *ACS Nano*, 9:11599–11607, 12 2015.

[56] G. H. Shirdel, H. Rezapour, and A. M. Sayadi. The hyper-zagreb index of graph operations. *Iranian journal of mathematical chemistry*, 4:213–220, 2013.

[57] K. Srogi. Monitoring of environmental exposure to polycyclic aromatic hydrocarbons: a review. *Environmental Chemistry Letters*, 5:169–195, 11 2007.

[58] Heinz A. Staab and François Diederich. Cycloarenes, a new class of aromatic compounds, i. synthesis of kekulene. *Chemische Berichte*, 116:3487–3503, 10 1983.

[59] Erich Steiner, Patrick W. Fowler, Angela Acocella, and Leonardus W. Jenneskens. Visualisation of counter-rotating ring currents in kekulene. *Chemical Communications*, pages 659–660, 2001.

[60] Damir Vukicevic and Marija Gaperov. Bond additive modeling 1. adriatic indices. *Croatica Chemica Acta*, 83:243–260, 2010.

[61] Damir Vukičević and Boris Furtula. Topological index based on the ratios of geometrical and arithmetical means of end-vertex degrees of edges. *Journal of Mathematical Chemistry*, 46:1369–1376, 11 2009.

[62] Jishan Wu, Wojciech Pisula, and Klaus Müllen. Graphenes as potential material for electronics. *Chemical Reviews*, 107:718–747, 3 2007.

[63] Kun Xu, José I. Urgel, Kristjan Eimre, Marco Di Giovannantonio, Ashok Keerthi, Hartmut Komber, Shiyong Wang, Akimitsu Narita, Reinhard Berger, Pascal Ruffieux, Carlo A. Pignedoli, Junzhi Liu, Klaus Müllen, Roman Fasel, and Xinliang Feng. On-surface synthesis of a nonplanar porous nanographene. *Journal of the American Chemical Society*, 141:7726–7730, 5 2019.

[64] Li Yan, Wei Gao, and Junsheng Li. General harmonic index and general sum connectivity index of polyomino chains and nanotubes. *Journal of Computational and Theoretical Nanoscience*, 12:3940–3944, 10 2015.

[65] Lei Zhang, Yang Cao, Nicholas S. Colella, Yong Liang, Jean-Luc Brédas, K. N. Houk, and Alejandro L. Briseno. Unconventional, chemically stable, and soluble two-dimensional angular polycyclic aromatic hydrocarbons: From molecular design to device applications. *Accounts of Chemical Research*, 48:500–509, 3 2015.

[66] Xiujun Zhang, H. M. Awais, M. Javaid, and Muhammad Kamran Siddiqui. Multiplicative zagreb indices of molecular graphs. *Journal of Chemistry*, 2019:1–19, 12 2019.

[67] Bo Zhou and Nenad Trinajstić. On a novel connectivity index. *Journal of Mathematical Chemistry*, 46:1252–1270, 11 2009.